International Journal of Engineering Trends and Technology
ISSN: 2231 – 5381 / https://doi.org/10.14445/22315381/IJETT-V70I6P207
Volume 70 Issue 6, 54-62, June 2022

Original Article

Sensor-less Monitoring of Induction Motor Temperature with an Online Estimation of Stator and Rotor Resistances Taking the Effect of Machine Parameters Variation into account

Bilal Abdullah Nasir

Northern Technical University, Iraq

bilalalnasir@ntu.edu.iq

Received: 23 March 2022 Revised: 20 May 2022 Accepted: 29 May 2022 Published: 27 June 2022

Abstract *- A novel and accurate method for induction motor online temperature monitoring based on stator and rotor winding thermal variation using the Arduino-Matlab Simulink technique is proposed and implemented in this paper. Estimating stator resistance as an indicator of stator winding and rotor bars temperature. Obtaining an accurate stator and rotor resistances is very important for this approach.*

A new determination of stator and rotor resistances for motor temperature monitoring in steady-state operation is proposed based on the motor dynamic model in a rotating reference frame. In this model, the effect of iron core losses is taken as a reflected voltage drop in the stator and rotor equivalent circuits. The skin and skew effect in the rotor circuit, stray load loss in stator and rotor circuits, variation effect in the magnetizing inductance, and variation in stator and rotor resistances are taken in this model to obtain an accurate temperature online monitoring. An experimental result on a line–connected induction motor satisfied the validity of the proposed model of analysis and method of motor temperature monitoring.

Keywords *- Temperature monitoring, Stator and rotor resistance estimation, Dynamic model, Iron core loss, Stray loss, Skin-effect, Skew effect.*

1. Introduction

Many failure resources of induction motors are caused by the breakdown of the stator winding insulation due to the thermal overloading. Therefore, the stator winding temperature must be monitored online to extend the insulation life and protect the motor under thermal overloading [1-2].

Due to the difficulty and expensive cost of installing thermal sensors inside the machine, the protection against thermal depends on fuses, thermal-overload relays, and electronic-overload relays, which have had fewer costs for many years. Recently, temperature estimation using microcontrollers with thermal models became available to compensate for the shortcoming of over-load relays [3]. Thermal models for temperature determination provide higher accuracy than overload relays but cannot respond to the change in thermal motor characteristics. The assumed fixed machine variables in the thermal model cannot respond to the temperature rise in case of abnormal conditions, such as a failure in the cooling system leading to a rapid motor failure.

The motor temperature estimators can be divided into two categories:

1. Offline Estimation: the variables of the induction machine are calculated offline by no-load test, blocked-rotor test, and load test. These methods are called variables identification methods.
2. Online Estimation: the motor variables are calculated during the conventional operation of the machine.

The offline temperature estimation models give poor accuracy due to the machine parameters being considered constant. In contrast, the online estimators give more accurate results than the offline estimators due to the effect of temperature variation on determining stator and rotor resistance. In online temperature calculation methods, there are five types of stator and rotor resistances estimation:

1. Zero sequence model by solving a least-squares minimization problem [4]. This technique achieves the machine parameters variation concerning zero sequence quantities.
2. DC. injection model is simply realizable for an online connected induction motor, but this model suffers from harmonic generation, which appears as torque pulsation ripple on the motor shaft [2].
3. 'Model Reference adaptive system (MRAS) estimators.' These estimators are proposed in [5-10]. The main drawback of these algorithms is that they need high-performance hardware to calculate the stator and rotor resistances values due to the need to

solve complex non-linear equations. The variation in motor parameters is not considered in these models.

4. The hybrid model is based on a fixed thermal model for less than 50% of a motor nominal load and machine parameters identification model for greater than 50% of motor nominal load to estimate the motor temperature [9]. This hybrid model cannot respond to the temperature rise in case of a failure in the cooling system, which leads to a rapid failure of the machine. Also, the parameters identification model ignores machine variable parameters such as magnetizing saturation, skin effect, and skew factor.
5. Induction machine dynamic model. This method does not require any external injection. It depends on motor parameters estimation, which is not linear and depends on operating conditions [10-18].

In [14], the rotor resistance estimation is based on a dynamic machine model and artificial neural network, considering the effect of skin (slip frequency). In [15], the rotor bar temperature estimation is based on a dynamic model of the machine and an indirect flux-oriented control algorithm. In [16], thermal monitoring of induction motor in steady-state online operation is based on the Estimation of rotor resistance in the dynamic electrical model. In contrast, the rotor speed is calculated from the dynamic mechanical model of the motor. This model omitted the magnetizing saturation, iron-core loss, stray-load loss, skin effect, and skew factor. In [17], an online estimation motor is presented, taking the effect of temperature variation. The magnetizing inductance is constant. The iron-core loss, stray loss, skin effect, and skew factor are also omitted in this model.

In [18] calculation of stator and rotor resistances is based on the computation of D-axis rotor flux linkage (λdr) in equation (19) of the model. Since the equation is wrong, the author attributes the poor accuracy and high error rate in calculating the stator resistance to the error rate in the determination of the rotor resistance, especially at very high speed (high frequency) of the motor because the calculation of the stator resistance depends on the calculation of the rotor resistance. The fact is that the calculation of the rotor resistance depends on the value of the magnetizing inductance, which is low at high speed after the motor reaches the state of magnetic saturation. The author believes that a high sensitivity in calculating stator resistance is caused by errors in calculating rotor resistance, magnetizing inductance, and leakage magnetic inductances. Also, there is an error in estimating the magnetic flux linkage of the stator and rotor, which is amplified due to the high frequency of the source (high speed of the motor), as well as the presence of an error rate in the measurement of the source voltage, line current, and motor speed, as the resistors calculations depend on these variables directly. It leads to the inability to correct Estimation and monitor the motor temperature. The main reason for a high error in calculating stator and rotor resistance is neglecting the effect of magnetic saturation in calculating the magnetic inductance and the skin and skew effect in calculating the rotor resistance. Also, neglecting the effect of stray losses in the motor and the error in equation (19) caused a high error rate in the calculation of the resistors and the Estimation of the motor temperature.

In [19] Indeed, considering the magnetic inductance constant during the motor operation leads to a certain error in estimating the resistances of the stator and rotor. Still, the author attributes the high error rate in the calculations to the constant magnetic, which is incorrect because an error causes a very high error rate in the equations of the dynamic model of the machine, especially equations (3, 4, 25) in that dynamic model. As the researcher used equations (3, 4) in his research to obtain a mathematical equation to calculate the rotor resistance from equation (14), and due to the error in equations (3, 4), the equation for calculating the rotor resistance (14) is incorrect. It is evident from Fig. (1) in that reference that the error rate reached 150% in calculating the error resistance. The other mistake is the use of equations (14-16) in calculating the resistance of the stator from Fig. (3).

For sensor-less temperature monitoring in the steady-state online operation of the induction motor, a new dynamical model of the machine is proposed. The model is considered in a synchronously rotating reference frame, considering all the machine parameters variation. The iron core temperature, stray loss temperature, magnetizing inductance saturation, skin effect, and skew effect are considered variable parameters. The rotor speed can be estimated from the dynamic mechanical model or measured online by measuring supply frequency, phase voltage, and phase current. The measured parameters can be fed to the Arduino controller with the computer Matlab Simulink to estimate the stator and rotor resistances and stator and rotor temperature variation online during the steady-state operation of the motor.

2. Determination of Stator and Rotor Winding Resistances Based on Dynamic Model

In [18, 19], it is confirmed that the dynamic model of the induction motor used in estimating the resistance of the stator and rotor cannot be used. It is due to the difficulty in obtaining acceptable accuracy in calculating stator and rotor resistance. It is confirmed by all references (researches) in this field through practical experiments, and there are no reasons that can be mentioned to diagnose the poor accuracy of the results obtained.

I believe that the main reason for the poor accuracy of the estimated results of stator and rotor resistances from the dynamic model is the use of all variables in the model as constants. It is incorrect because the machine variables vary during the operation, which must be considered. In addition, neglecting many variables and not entering them within the model, such as the effect of the skin phenomenon, skew, magnetic saturation, iron core losses, and stray losses.

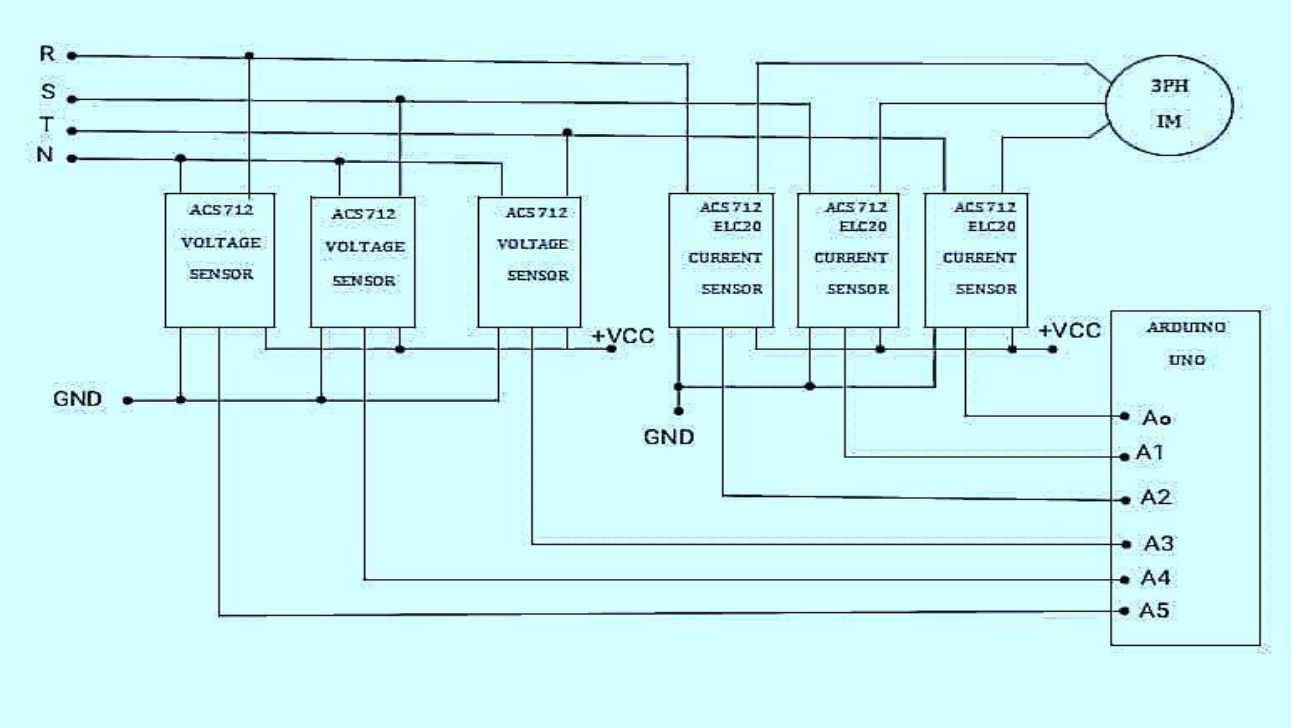

Fig. 1 Schematic of the 3-phase induction motor-Arduino controller system

Figure (1) shows the diagram of the 3-phase induction motor-Arduino controller system. The Arduino is connected online with the motor through ACS-712 type voltage and current sensors, while the motor is connected to the supply without interior temperature sensors.

In the current dynamic model of the figure (2), all the motor parameters will be entered into the model to obtain high accuracy in calculating the motor resistances on which the machine temperature calculations depend directly. The following motor parameters can be considered in the dynamic model:

2.1. Resistances of iron core

The iron core resistance is varied with the temperature and air-gap magnetizing voltage and calculated from the no-load test of the motor as [20]:

$$R_{ic} = V_g^2 \,/\, [K_T * (P_{n\ell} - I_o^2 * R_s)] \quad (1)$$

$$V_g = X_m * I_m = X_m * I_o * \sin(\phi_o) \quad (2)$$

$$I_m = \left[\frac{Q_{n\ell} - I_o^2 * X_{\ell s}}{X_m}\right]^{\frac{1}{2}} \quad (3)$$

where V_g is the air-gap or magnetizing voltage per phase and can be calculated in terms of magnetizing reactance (X_m), no-load current (I_o) and no-load sine of power factor angle ($\sin(\phi_o)$) The iron core resistance was obtained in terms of air-gap magnetizing voltage as given in appendix-A.

K_T= (1-D) is the temperature coefficient of the iron core loss.

D is the iron core power loss varying rate per ^oC and can be determined as [20]:

$$D = \left[P_{ic\,(To)} - P_{ic\,(T)}\right] / P_{ic\,(To)} \quad (4)$$

where $P_{ic\,(To)}$ is the iron core power loss at ambient temperature, and $P_{ic\,(T)}$ is the iron core power loss at any temperature. These iron core power losses are measured from the no-load test of the motor.

$P_{n\ell}$ is the active no-load power loss per phase.

$R_{so}$is the stator resistance per phase at ambient temperature.

$Q_{n\ell}$ is the reactive no-load power loss per phase.

$X_{\ell s}$is the stator leakage reactance per phase.

The resistance (R_{ic}) of the iron core can be referred to on the stator and rotor circuits as a voltage drop to stay the dynamic model order fixed on the 4th order, while the effect of iron core loss is considered as shown in figure (1). The reflecting resistance on the stator circuit (R_{ssic}) and the reflecting resistance of iron core on the rotor circuit (R_{rsic}) calculated as [21]:

$$R_{ssic} = (R_{sic} * \omega_s * L_M) \,/\, [R_{sic}^2 + (\omega_s + L_M)^2] \quad (5)$$

$$R_{rsic} = s * R_{ssic} \quad (6)$$

Where R_{sic} is the stator iron core resistance and calculated as:

$$R_{sic} = R_{ic} * (\omega_s * L_M)^2 \,/\, [R_{ic}^2 + (\omega_s * L_M)^2] \quad (7)$$

Where L_M is the magnetizing inductance per phase and can be obtained from the no-load test as:

$$L_M = X_m / \omega_s \quad (8)$$

$\omega_s = (2 * \pi * f)$ is the angular frequency in rad. / sec.

The modified magnetizing inductance (L_m) in figure (1) of the dynamic model can be calculated as:

$$L_m = L_M * R_{ic}^2 / [R_{ic}^2 + (\omega_s * L_M)^2] \quad (9)$$

2.2. Stray loss resistances

The stray load loss resistances can be varied with the variation of stator and rotor resistances due to the temperature variation. These resistances can be calculated and introduced in the dynamic model, as shown in figure (2). These resistances are obtained and given as series resistances in the stator and rotor circuits [22]:

$$R_{sss\ell} = (\omega_s * L_{\ell s})^2 * R_s / [R_s^2 + (\omega_s * L_{\ell s})^2] \quad (10)$$

$$R_{rss\ell} = S^2 * (\omega_s * L'_{\ell r})^2 / R'_r \quad (11)$$

Where $R_{sss\ell}$ and $R_{rss\ell}$are motor stator and rotor series stray-load loss resistances, respectively.

S is the motor slip and $L_{\ell r}$ is the rotor leakage inductance per phase.

2.3. Include magnetizing saturation

All induction machines operate in the saturation region, and their characteristics are non-linear. The variation of magnetizing reactance (X_m) is the main factor in producing the magnetizing air-gap voltage (V_g).

The magnetizing air-gap voltage is the main factor in producing iron-core losses, rotor current, mechanical losses, and output power. The saturation reduces V_g And tends to increase. The saturation - the effect is taken by the relation $X_m = f(I_m)$.

This function can be obtained experimentally from the no-load test by varying supply voltage from 125% to 25% of the rated value. Then the measurements of X_m and I_m can be interpolated by the curve fitting technique [20] as given in appendix-A.

2.4. Correction factors

1. The skew factor can correct the rotor phase leakage reactance (K_{sq}) [23]:

$$\acute{X}_{\ell r} = \frac{X_m}{K_{sq}^2}\left(1 - K_{sq}^2\right) + \frac{\acute{X}_{\ell r}}{K_{sq}^2} \quad \text{total rotor leakage reactance} \quad (12)$$

$$K_{sq} = sin\left(\frac{\pi * P_p}{Q_r}\right) / \left(\pi * P_p / Q_r\right) \quad \text{rotor skew factor} \quad (13)$$

Where P_p is the machine magnetic pole-pairs Q_r is the number of rotor slots (bars).

2. The rotor phase resistance can be corrected by the skew factor as :

$$\acute{R}_r = \acute{R}_r / K_{sq}^2 \quad (14)$$

3. The skin effect can correct the rotor phase resistance and leakage reactance as [21] :

$$\acute{\acute{R}}_r = \acute{R}_r * \left[\, 0.5 + 0.5 * \sqrt{S_r / S_m}\, \right] \quad (15)$$

$$\acute{\acute{X}}_{\ell r} = \acute{X}_{\ell r} * \left[\, 0.4 + 0.6 * \sqrt{S_m / S_r}\, \right] \quad (16)$$

Where S_r is the rated machine slip and S_m is the machine slip at maximum torque and can be given as [21]:

$$S_m = \acute{R}_r / \left[(R_s + R_{sss\ell})^2 + (X_{\ell s} + \acute{X}_{\ell r})^2\right]^{½} \quad (17)$$

Also, the machine slip can be corrected due to the temperature effect as [23]:

$$\acute{S}_{r,m} = S_{r,m} * (T_r + K_a) / (T_{ref} + K_a) \quad (18)$$

where T_r is the rotor bar temperature at any load and T_{ref} is the temperature of insulation class level and can be obtained from the table of insulation class.
K_a is constant and equal to (225) for aluminum rotor bar type.

The dynamic electrical equations of the induction motor are obtained from the proposed equivalent circuit in figure (2) as:

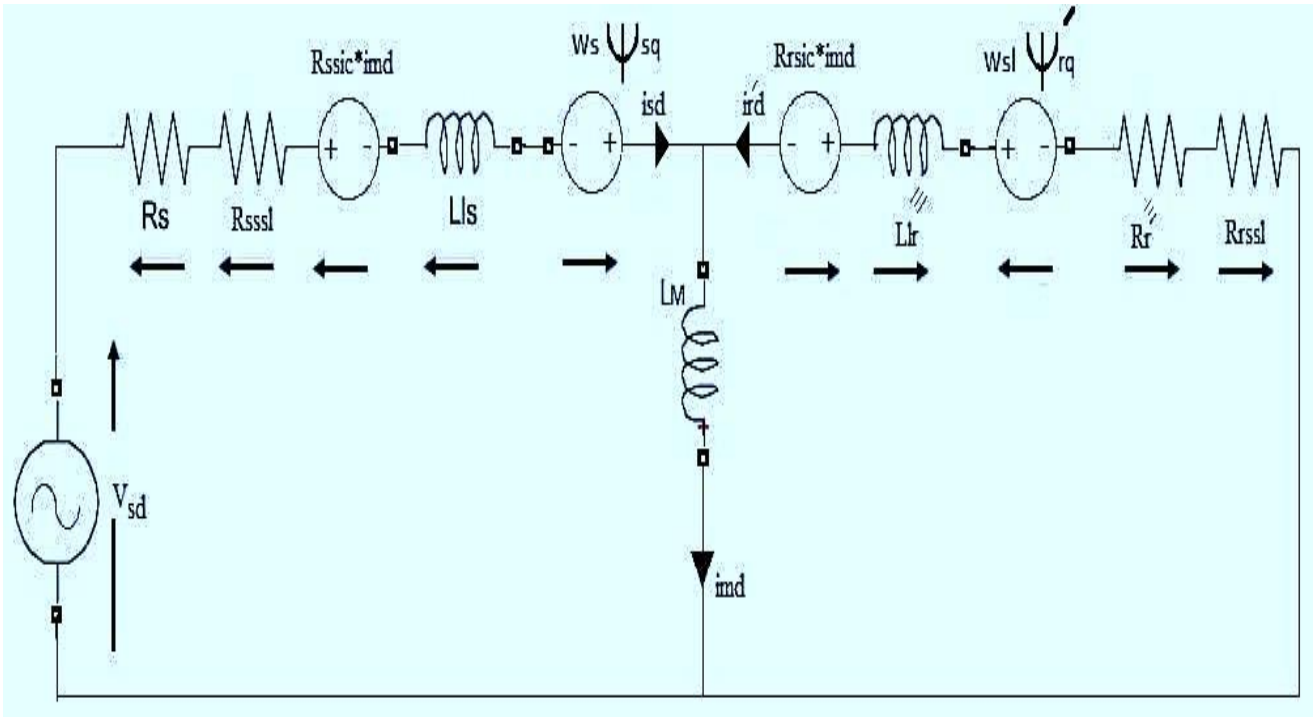

(a) D-axis equivalent circuit model

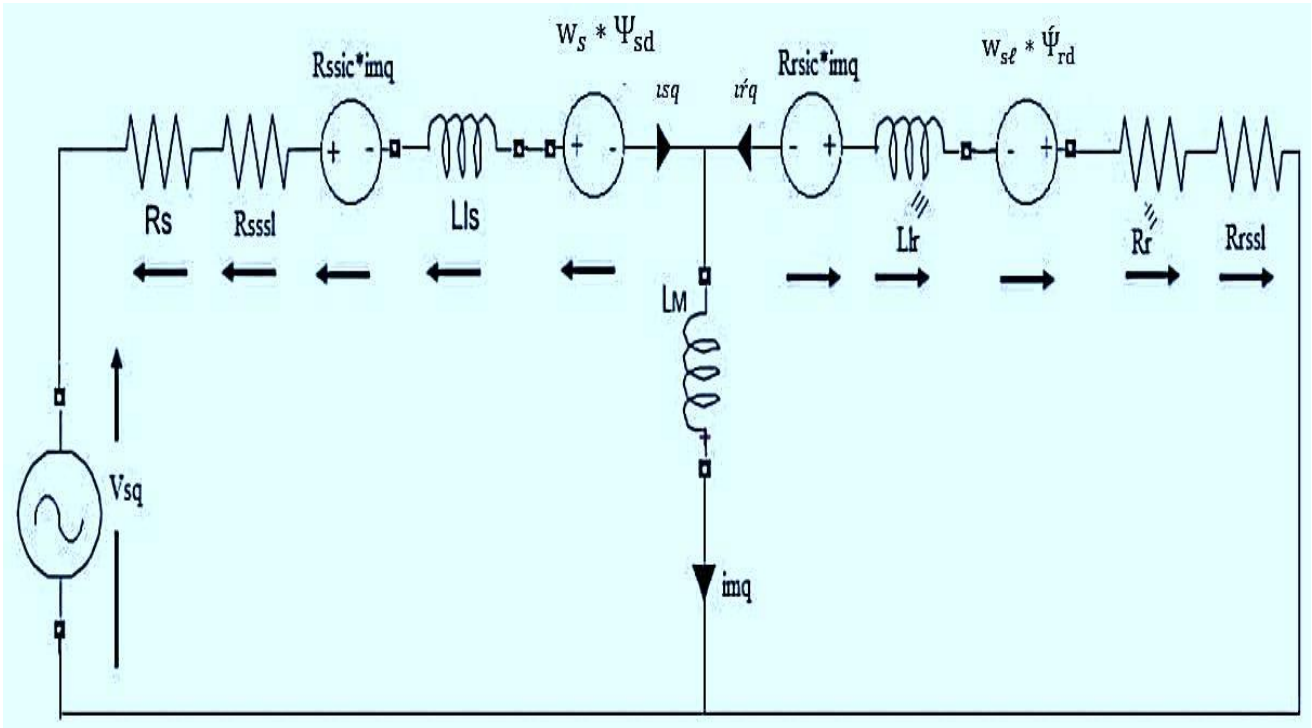

(b) Q-axis equivalent circuit model

Fig. 2 D-Q axes of the proposed equivalent circuit in the synchronously rotating frame

$$v_{sd} = (R_s + R_{sss\ell})\, i_{sd} + R_{ssic}\, i_{md} - \omega_s \psi_{sq} + \frac{d\psi_{sd}}{dt} \quad (19)$$

$$v_{sq} = (R_s + R_{sss\ell})\, i_{sq} + R_{ssic}\, i_{mq} + \omega_s \psi_{sd} + \frac{d\psi_{sq}}{dt} \quad (20)$$

$$o = \left(\acute{\acute{R}}_r + R_{rss\ell}\right) \acute{\imath}_{rd} + R_{rsic}\, \acute{\imath}_{md} - \omega_{s\ell}\, \acute{\psi}_{rq} + \frac{d\acute{\psi}_{rd}}{dt} \quad (21)$$

$$o = \left(\acute{\acute{R}}_r + R_{rss\ell}\right) \acute{\imath}_{rq} + R_{rsic}\, \acute{\imath}_{mq} + \omega_{s\ell}\, \acute{\psi}_{rd} + \frac{d\acute{\psi}_{rq}}{dt} \quad (22)$$

Where $\omega_{s\ell} = \omega_s - \omega_r = s * \omega_s$ Slip speed in electrical. rad. / sec.

$\omega_r = P_p * \omega_m$ is the electrical angular speed of the motor in (electrical . radian/sec.)

$\psi_{sd}, \psi_{sq}, \acute{\psi}_{rd}$ and $\acute{\psi}_{rq}$ are the stator and rotor flux linkages in D-Q axes, respectively, defined as :

$$\psi_{sd} = L_{\ell s} * i_{sd} + L_m * i_{md} \quad (23)$$

$$\psi_{sq} = L_{\ell s} * i_{sq} + L_m * i_{mq} \quad (24)$$

$$\acute{\psi}_{rd} = \acute{\acute{L}}_{\ell r} * \acute{\imath}_{rd} + L_m * i_{md} \quad (25)$$

$$\acute{\psi}_{rq} = \acute{\acute{L}}_{\ell r} * \acute{\imath}_{rq} + L_m * i_{mq} \quad (26)$$

Equations (19-22) can be transformed by making the D-axis rotating frame coincide and rotating synchronously with the D-axis stator current (i_{sd}). It makes the Q-axis stator current (i_{sq}) equal to zero ($i_{sq} = 0$). Then, by assuming steady-state operation conditions, this leads to making the derivative of flux linkages in the D-Q axes $\left(\frac{d\psi_{sd}}{dt}, \frac{d\psi_{sq}}{dt}, \frac{d\acute{\psi}_{rd}}{dt}, \frac{d\acute{\psi}_{rq}}{dt}\right)$ equal to zero, and by substituting equations (23-26) into (19-22) and further reduced to obtain the following equations :

$$\nu_{sd} = (R_s + R_{sss\ell} + R_{ssic})\, i_{sd} + R_{ssic} * \acute{\imath}_{rd} - \omega_s * L_m * \acute{\imath}_{rq} \quad (27)$$

$$\nu_{sq} = \omega_s * (L_{\ell s} + L_m) * i_{sd} + \omega_s * L_m * \acute{\imath}_{rd} \quad (28)$$

$$o = R_{rsic} * i_{sd} + \left(\acute{\acute{R}}_r + R_{rss\ell} + R_{rsic}\right) * \acute{\imath}_{rd} + \omega_{s\ell} * \left(\acute{\acute{L}}_{\ell r} + L_m\right) \acute{\imath}_{rq} \quad (29)$$

$$o = \omega_{s\ell} * L_m * i_{sd} + \omega_{s\ell} * \left(\acute{\acute{L}}_{\ell r} + L_m\right) * \acute{\imath}_{rd} + \left(\acute{\acute{R}}_r + R_{rss\ell} + R_{rsic}\right) * \acute{\imath}_{rq} \quad (30)$$

In equations (27-30), assuming $L_s = (L_{\ell s} + L_m)$ is the stator self-inductance and $L_r = \left(\acute{\acute{L}}_{\ell r} + L_m\right)$ Is the rotor self-inductance. Then solve these equations to get an expression for stator phase resistance ($R_{s(t)}$) and rotor phase resistance $\left(\acute{\acute{R}}_{r(t)}\right)$ in terms of motor phase voltage, motor phase current, and rotor speed (ω_r) as:

$$\acute{\acute{R}}_{r(t)} = \omega_{s\ell} * L_m * \left[\frac{\omega_s * L_r}{\left(\omega_s * L_s - \frac{\nu_{sq}}{i_{sd}}\right)} - \frac{L_r^2}{L_m^2}\right]^{1/2} - (R_{rss\ell} + R_{rsic}) \quad (31)$$

$$R_{s(t)} = \frac{\nu_{sd}}{i_{sd}} + \left[\frac{(\acute{\acute{R}}_r + R_{rss\ell} + R_{rsic})}{(\omega_{s\ell} * L_r)} * \left(\frac{\nu_{sq}}{i_{sd}} - \omega_s * L_s\right)\right] - (R_{sss\ell} + R_{ssic}) \quad (32)$$

The rotor mechanical speed (ω_m)can be calculated from the dynamic mechanical model as :

$$\frac{d\omega_m}{dt} = \frac{1}{J}\left(T_e - T_\ell - V_f * \omega_m\right) \quad (33)$$

Where T_e is the electromagnetic torque of the motor and can be calculated as [21]:

$$T_e = \left(\frac{3}{2}\right) * P_p * L_m * (i_{sd} * \acute{\imath}_{rq} - i_{sq} * \acute{\imath}_{rd}) \quad (34)$$

T_ℓ is the motor load torque in (N . m).

J is the moment of inertia in ($K_g \,.\, m^2$).

P_p is the magnetic pole-pairs number.

V_f is the viscosity resistance factor N.m / (rad. / sec.) .

The magnetizing inductance (L_m) in terms of magnetizing current (I_m) from the no-load test can be introduced in the dynamic model as a polynomial curve fitting to consider magnetizing saturation.

$i_{sq} = o$, due to the D-axis frame coinciding with the D-axis stator current (i_d).

i_{sd} is the measured phase current.

$$\acute{\imath}_{rd} = \left(\nu_{sq} - \omega_s * L_s * i_{sd}\right) / (\omega_s * L_m) \quad (35)$$

$$i_{md} = i_{sd} + \acute{\imath}_{rd} \quad (36)$$

$$\acute{\imath}_{rq} = \frac{[-\nu_{sd} + (R_s + R_{sss\ell}) * i_{sd} + R_{ssic} * i_{md}]}{(\omega_s * L_m)} \quad (37)$$

$$i_{mq} = i_{sq} + \acute{\imath}_{rq} \quad (38)$$

$$I_m = \sqrt{i_{md}^2 + i_{mq}^2} / \sqrt{2} \quad (39)$$

3. Sensorless Online Monitoring Motor Winding Temperature

In the absence of temperature sensors, it is preferred to calculate the variation in the motor resistances during the normal steady-state operation. Then the stator and rotor winding temperature is calculated online at any load and operating time as [24]:

$$T_s = T_a + \frac{(R_{s(t)} - R_s)}{\propto_s * R_s} \quad (40)$$

$$T_r = T_a + \frac{\left(\acute{\acute{R}}_{r(t)} - \acute{R}_r\right)}{\propto_r * \acute{R}_r} \quad (41)$$

Where $R_{r(t)}$ and $R_{s(t)}$ are the calculated rotor and stator resistance from equation (31-32).

R_r and R_s are the rotor and stator resistances at ambient temperature (25℃).

$\propto_r$ and $\propto_s$ are the temperature coefficients of the rotor and stator winding materials type ($\propto_r = 0.004$, $\propto_s = 0.0039$).

For comparison of the results of this method, the stator and rotor winding temperature can be calculated at any online operating time from the following relations [25]:

$$T_s = \frac{I_s^2}{I_{sf\ell}^2}\left(T_{ref} - T_a\right) + T_a \quad (42)$$

$$T_r = \frac{(I_s - I_o)^2}{(I_{sf\ell} - I_o)^2}\left[T_{ref} - T_a\right] + T_a \quad (43)$$

Where I_s = stator current per phase at any load.

$I_{sf\ell}$ = stator current per phase at full load from the machine's nameplate.

I_o = stator no-load current per phase.

T_{ref} = reference temperature depends on the class of insulation system(Appendix-B).

T_a = ambient temperature (25℃).

4. Result and Discussion

The test bench consists of an induction 3-phase induction motor connected with an Arduino controller on a 3-phase A.C. supply to estimate the motor stator winding and rotor bar temperature variation online without sensors during any operating time and load conditions. The motor specifications are given in appendix-A

The Arduino controller type UNO with voltage and current sensors type ACS 712.

The dynamic model of the motor is fed to the Arduino controller as a code (program) to calculate the rotor and then stator phase resistance, and the stator winding and rotor bar temperature can be determined.

Figure (3) shows the online variation of stator winding and rotor bar resistances with time during the motor operation. The percentage variation of these resistances is about 20% for the rotor bars and 12% for stator winding during 90 minutes of continuous motor operation. Figure (4) shows the variation of stator winding and rotor bar temperature with time during 90 minutes of continuous motor operation. The rotor bar temperature is nearly 10 ℃ above the stator coil temperature.

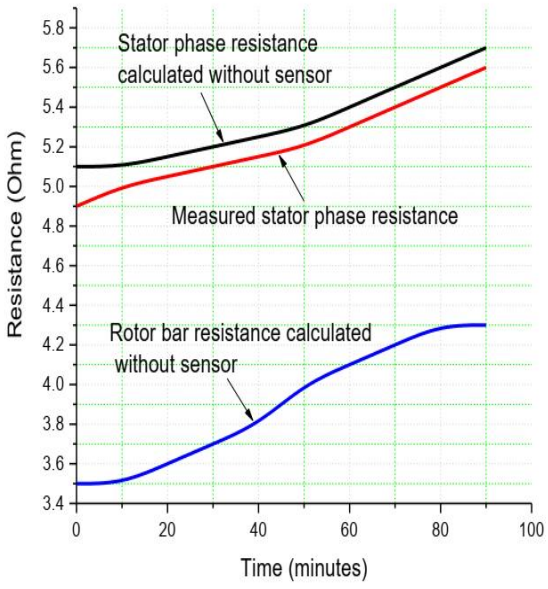

Fig. 3 Resistance variation with time

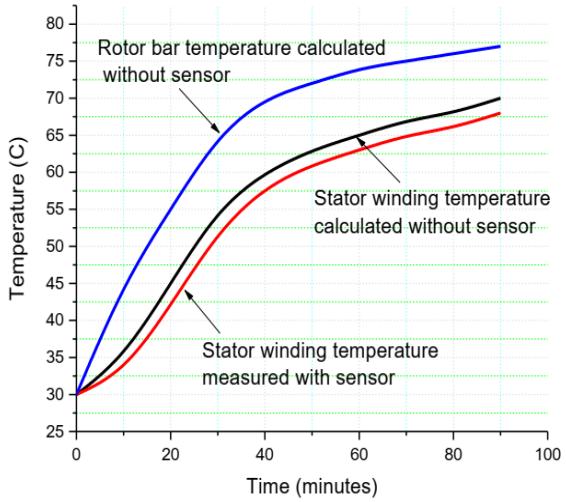

Fig. 4 Temperature variation with time

5. Conclusion

A new and efficient method is proposed for accurate and sensor-less online monitoring of induction motor temperature during continuous operation in steady-state conditions. The accurate dynamic model of the induction motor is fed to the Arduino programmable controller as a code (program). The main parameters of calculation (phase voltage and current) are measured directly online by voltage and current sensors and then fed to the controller to calculate the rotor and stator phase resistances and their temperatures online.

The error in estimating rotor and stator resistances is minimized due to the flux saturation and skin effect considered in the dynamic model. The iron core loss, stator copper loss, and rotor copper loss are considered heat sources.

Appendix

The induction machine specification and parameters are given as follows:

3-Phase, squirrel cage, $\Delta - connected$, 220 V line voltage, 50 Hz, has the following parameters :

$$P_{out} = 1500\ W, N_s = 1500\ r.p.m\ , I_\ell = 6.6\ A\ , P_p = 2, Cos\ (\phi) = 0.8,$$
$$R_s = 5.1\ \Omega, \acute{R}_r = 3.5\ \Omega, L_{\ell s} = 16\ mH\ , \acute{L}_{\ell r} = 24\ mH\ , L_M = 0.28\ H\ ,$$

$R_{ic} = 280\ \Omega\ at\ rated\ voltage\ , J = 0.025\ Kg.m^2\ , V_f = 0.002\ N.m/(rad./sec.)$ Viscosity resistance factor, $R_{f\omega} = 1660\ \Omega$, friction, and windage loss resistance, $T_{f\ell} = 10\ N.m$ full load torque, I_0 = 1.0 A

Design class-B, Insulation class-F, $K_T = 0.75$ temperature coefficient of iron core loss, $\propto_r = 0.004\ and\ \propto_s = 0.0039$ temperature coefficient of stator and rotor material type, the magnetizing inductance as a function of magnetizing current (I_m) is obtained as:

$$L_M = 0.0476 * I_m^5 - 0.513 * I_m^4 + 2.18 * I_m^3 - 4.57 * I_m^2 + 4.63 * I_m + 0.25$$
$$R_{ic} = -0.0001985 * V_g^3 + 0.111 * V_g^2 - 23.11 * V_g + 840$$

The table of insulation class levels is given as [24]

Insulation class level	Rated or reference temperature $T_{ref.}$(℃)
A	75
B	95
F	115
H	130

The table of design classes is given as [24]

Design class	$X_{\ell s}/\acute{X}_{\ell r}$ ratio
A, D, and wound rotor machine	1.0 $(X_{\ell s} = \acute{X}_{\ell r})$
B	0.67 $(X_{\ell s} = 0.67 * \acute{X}_{\ell r})$
C	0.43 $(X_{\ell s} = 0.43 * \acute{X}_{\ell r})$

References

[1] K.D. Hurst and T.G. Habetler, Thermal Monitoring and Parameter Tuning Scheme for Induction Machines, Conference Rec. IEEE-IAS Annual Meeting. 1 (1994) 776-784.

[2] D. A. Paice, Motor Thermal Protection by Continuous Monitoring of Winding Resistance, IEEE Transactions on Ind. Elect. Instrumentation. IECI-27 (1980) 137-141. Doi:10.1109/TIECI.1980.351666

[3] S. B. Lee and T.G. Habetler, An Online Stator Winding Resistance Estimation Technique for Temperature Monitoring of Line-Connected Induction Machine, IEEE Transactions on Industry Applications. 39(3) (2003) 685-694. Doi: 10.1109/TIA.2003.811789.

[4] C. B. Jacobina, J.E.C. Filho and A.M.N. Lima, Online Estimation of Stator Resistance of Induction Machines on Zero Sequence Model, IEEE Transaction on Power Electronics. 15(2) (2000) 346-353. Doi: 10.1109/63.838107.

[5] C. Kral, et al., Rotor Temperature Estimation of Squirrel-Cage Induction Motors Utilizing a Combined Scheme of Parameter Estimation and a Thermal Equivalent Model, IEEE, Transactions on Industry Applications. 40(4) (2004) 1049-1057. Doi: 10.1109/TIA.2004.830759.

[6] (2006). Zhi Gao, Sensorless Stator Winding Temperature Estimation for Induction Machines, Doctoral Thesis, Georgia Institute of Technology. [Online]. Available: https://smartech.gatech.edu/bitstream/handle/1853/13966/gao_zhi_200612_phd.pdf

[7] Maximiliano O. Sonnaillon, Guillermo Bisheimer, Cristian De Angelo, and Guillermo O. Garc´ıa, Online Sensorless Induction Motor Temperature Monitoring, IEEE Transactions on Energy Conversion. 25(2) (2010) 273-280. https://www.academia.edu/6877600/

[8] B.Das, A. Chakrabarti, P.R.Kasari and N.Sharma, Sensorless Speed Control of DC Machine, International Conference on Power, Energy and Control ICPEC. (2013) 572-577. Doi: 10.1109/ICPEC.2013.6527723.

[9] S. A. Bednarz and M. Dybkowski, Estimation of the Induction Motor Stator and Rotor Resistance Using Active and Reactive Power-Based Model Reference Adaptive System (MRAS) Estimator, Applied Science Journal, MDPI. 23(5145) (2019) 1-19. https://doi.org/10.3390/app9235145

[10] F.L. Mapelli, D. Tarsitano, and F. Cheli, MRAS Rotor Resistance Estimators for E.V. Vector Controlled Induction Motor Traction Drive: Analysis and Experimental Results, Electric Power Systems Research, Elsevier Publisher. 146 (2017) 298-307. https://isiarticles.com/bundles/Article/pre/pdf/146200.pdf.

[11] M. Sivakumar, T. Thanakodi and N. Panneer Selvam, Comparative Analysis of Stator Resistance Estimators in DTC-CSI Fed I.M. Drive, International Journal of Applied Engineering Research. 13(15) (2018) 12364-12372. https://www.ripublication.com/ijaer18/ijaerv13n15_92.pdf

[12] Mingyu Wang et al., Simplified Rotor and Stator Resistance Estimation Method Based on Direct Rotor Flux Identification, Journal of Power Electronics. 19(3) (2019) 751-760.

[13] Nikbakhsh, H.R. Izadfar, and M. Jazaeri, Classification and Comparison of Rotor Temperature Estimation Methods of Squirrel Cage Induction Motors, Journal of Measurement, Elsevier Publisher. 145 (2019) 779-802. https://www.sciencedirect.com/science/article/abs/pii/S0263224119303057?via%3Dihub

[14] Fan, Z. Yang, W. Xu and X. Wang, Rotor Resistance Online Identification of Vector Controlled Induction Motor Based on the Neural Network, Journal of Mathematical Problems in Engineering, Hindawi Publishing Corporation. 2014(831839) (2014) 1-10. https://doi.org/10.1155/2014/831839

[15] Tuan-Vu Tran and E. Negre, Efficient Estimator of Rotor Temperature Designing for Electric and Hybrid Powertrain Platform, Journal of Electronic. 9(1096) (2020) 1-12. https://doi.org/10.3390/electronics9071096

[16] R. Beguenane and M. E. H. Benbouzid, Induction Motor Thermal Monitoring Utilizing Rotor Resistance Identification, IEEE Transaction on Energy Conversion. 14(3) (1999) 566-570. Doi: 10.1109/60.790915.

[17] P. Blaha and P. Vaclavek, A.C. Induction Motor Stator Resistance Estimation Algorithm, 7th WSEAS International Conference on Electric Power System, High Voltages, Electric Machines, Venice, Italy, Corpus ID: 29248773. 86-91 (2007) 21-23 .

[18] S. B. Lee, T.G. Habetler, R.G. Harley and D.J. Gritter, A Stator and Rotor Resistance Estimation Technique for Conductor Temperature Monitoring, Conference Rec. IEEE-IAS Annual Meeting. 1 (2000) 381-387.

[19] S. B. Lee, T.G. Habetler, R. G. Harley and D. J. Gritter, An Evaluation of Model-Based Stator Resistance Estimation for Induction Motor Stator Winding Temperature Monitoring, IEEE Transactions on Energy Conversion. 17(1) (2002) 7-15. Doi: 10.1109/MPER.2002.4311669

[20] B. A. Nasir, An Accurate Iron Core Loss Model in the Equivalent Circuit of Induction Machines, Journal of Energy, Hindawi Publisher, Article ID 7613737. (2020) 1-10. https://www.hindawi.com/journals/jen/2020/7613737/

[21] B. A. Nasir and R. W. Daoud, Modeling of Wind Turbine-Self Excited Induction Generator System with Pitch Angle and Excitation Capacitance Control, AIP Conference Proceedings. 2307(1) (2020) 1-21. https://aip.scitation.org/doi/abs/10.1063/5.0032904

[22] B. A. Nasir, Modeling of Stray Losses in the Equivalent Circuit of Induction Machines, AIP Conference Proceedings. 2307(1) (2020) 1-11. https://aip.scitation.org/doi/10.1063/5.0032902

[23] B. A. Nasir, An Accurate Determination of Induction Machine Equivalent Circuit Components, Proceedings of the 1st International Multi-Disciplinary Conference Theme: Sustainable Development and Smart Planning IMDC-SDSP, Cyberspace. (2020) 28-30.

[24] IEEE Power Engineering Society, IEEE Standard Test Procedure for Polyphase Induction Motors and Generators, ANSI, IEEE Standard. 112-B (2004). Doi: 10.1109/IEEESTD.1991.114383.

[25] B. A. Nasir, Modeling of a Self-Excited Induction Generator in the Synchronously Rotating Frame Including Dynamic Saturation and Iron Core Loss Into Account, International Journal of Electrical and Computer Sciences. 20(1) (2020) 1-6. http://ijens.org/Vol_20_I_01/202401-4747-IJECS-IJENS.pdf